Strange Baryon Resonance Production in $\sqrt{s_{NN}} = 200$ GeV $p + p$ and Au + Au Collisions

B. I. Abelev,[50] M. M. Aggarwal,[30] Z. Ahammed,[45] J. Amonett,[20] B. D. Anderson,[20] M. Anderson,[6] D. Arkhipkin,[13] G. S. Averichev,[12] Y. Bai,[28] J. Balewski,[17] O. Barannikova,[9] L. S. Barnby,[2] J. Baudot,[18] S. Bekele,[29] V. V. Belaga,[12] A. Bellingeri-Laurikainen,[40] R. Bellwied,[48] F. Benedosso,[28] S. Bhardwaj,[35] A. Bhasin,[19] A. K. Bhati,[30] H. Bichsel,[47] J. Bielcik,[50] J. Bielcikova,[50] L. C. Bland,[3] S-L. Blyth,[22] B. E. Bonner,[36] M. Botje,[28] J. Bouchet,[40] A. V. Brandin,[26] A. Bravar,[3] T. P. Burton,[2] M. Bystersky,[11] R. V. Cadman,[1] X. Z. Cai,[39] H. Caines,[50] M. Calderón de la Barca Sánchez,[6] J. Castillo,[28] O. Catu,[50] D. Cebra,[6] Z. Chajecki,[29] P. Chaloupka,[11] S. Chattopadhyay,[45] H. F. Chen,[38] J. H. Chen,[39] J. Cheng,[43] M. Cherney,[10] A. Chikanian,[50] W. Christie,[3] J. P. Coffin,[18] T. M. Cormier,[48] M. R. Cosentino,[37] J. G. Cramer,[47] H. J. Crawford,[5] D. Das,[45] S. Das,[45] S. Dash,[15] M. Daugherity,[42] M. M. de Moura,[37] T. G. Dedovich,[12] M. DePhillips,[3] A. A. Derevschikov,[32] L. Didenko,[3] T. Dietel,[14] P. Djawotho,[17] S. M. Dogra,[19] W. J. Dong,[7] X. Dong,[38] J. E. Draper,[6] F. Du,[50] V. B. Dunin,[12] J. C. Dunlop,[3] M. R. Dutta Mazumdar,[45] V. Eckardt,[24] W. R. Edwards,[22] L. G. Efimov,[12] V. Emelianov,[26] J. Engelage,[5] G. Eppley,[36] B. Erazmus,[40] M. Estienne,[18] P. Fachini,[3] R. Fatemi,[23] J. Fedorisin,[12] K. Filimonov,[22] P. Filip,[13] E. Finch,[50] V. Fine,[3] Y. Fisyak,[3] J. Fu,[49] C. A. Gagliardi,[41] L. Gaillard,[2] M. S. Ganti,[45] L. Gaudichet,[40] V. Ghazikhanian,[7] P. Ghosh,[45] J. E. Gonzalez,[7] Y. G. Gorbunov,[10] H. Gos,[46] O. Grebenyuk,[28] D. Grosnick,[44] S. M. Guertin,[7] K. S. F. F. Guimaraes,[37] N. Gupta,[19] T. D. Gutierrez,[6] B. Haag,[6] T. J. Hallman,[3] A. Hamed,[48] J. W. Harris,[50] W. He,[17] M. Heinz,[50] T. W. Henry,[41] S. Hepplemann,[31] B. Hippolyte,[18] A. Hirsch,[33] E. Hjort,[22] A. M. Hoffman,[23] G. W. Hoffmann,[42] M. J. Horner,[22] H. Z. Huang,[7] S. L. Huang,[38] E. W. Hughes,[4] T. J. Humanic,[29] G. Igo,[7] P. Jacobs,[22] W. W. Jacobs,[17] P. Jakl,[11] F. Jia,[21] H. Jiang,[7] P. G. Jones,[2] E. G. Judd,[5] S. Kabana,[40] K. Kang,[43] J. Kapitan,[11] M. Kaplan,[8] D. Keane,[20] A. Kechechyan,[12] V. Yu. Khodyrev,[32] B. C. Kim,[34] J. Kiryluk,[23] A. Kisiel,[46] E. M. Kislov,[12] S. R. Klein,[22] A. Kocoloski,[23] D. D. Koetke,[44] T. Kollegger,[14] M. Kopytine,[20] L. Kotchenda,[26] V. Kouchpil,[11] K. L. Kowalik,[22] M. Kramer,[27] P. Kravtsov,[26] V. I. Kravtsov,[32] K. Krueger,[1] C. Kuhn,[18] A. I. Kulikov,[12] A. Kumar,[30] A. A. Kuznetsov,[12] M. A. C. Lamont,[50] J. M. Landgraf,[3] S. Lange,[14] S. LaPointe,[48] F. Laue,[3] J. Lauret,[3] A. Lebedev,[3] R. Lednicky,[13] C-H. Lee,[34] S. Lehocka,[12] M. J. LeVine,[3] C. Li,[38] Q. Li,[48] Y. Li,[43] G. Lin,[50] X. Lin,[49] S. J. Lindenbaum,[27] M. A. Lisa,[29] F. Liu,[49] H. Liu,[38] J. Liu,[36] L. Liu,[49] Z. Liu,[49] T. Ljubicic,[3] W. J. Llope,[36] H. Long,[7] R. S. Longacre,[3] W. A. Love,[3] Y. Lu,[49] T. Ludlam,[3] D. Lynn,[3] G. L. Ma,[39] J. G. Ma,[7] Y. G. Ma,[39] D. Magestro,[29] D. P. Mahapatra,[15] R. Majka,[50] L. K. Mangotra,[19] R. Manweiler,[44] S. Margetis,[20] C. Markert,[42] L. Martin,[40] H. S. Matis,[22] Yu. A. Matulenko,[32] C. J. McClain,[1] T. S. McShane,[10] Yu. Melnick,[32] A. Meschanin,[32] J. Millane,[23] M. L. Miller,[23] N. G. Minaev,[32] S. Mioduszewski,[41] C. Mironov,[20] A. Mischke,[28] D. K. Mishra,[15] J. Mitchell,[36] B. Mohanty,[45] L. Molnar,[33] C. F. Moore,[42] D. A. Morozov,[32] M. G. Munhoz,[37] B. K. Nandi,[16] C. Nattrass,[50] T. K. Nayak,[45] J. M. Nelson,[2] P. K. Netrakanti,[45] L. V. Nogach,[32] S. B. Nurushev,[32] G. Odyniec,[22] A. Ogawa,[3] V. Okorokov,[26] M. Oldenburg,[22] D. Olson,[22] M. Pachr,[11] S. K. Pal,[45] Y. Panebratsev,[12] S. Y. Panitkin,[3] A. I. Pavlinov,[48] T. Pawlak,[46] T. Peitzmann,[28] V. Perevoztchikov,[3] C. Perkins,[5] W. Peryt,[46] S. C. Phatak,[15] R. Picha,[6] M. Planinic,[51] J. Pluta,[46] N. Poljak,[51] N. Porile,[33] J. Porter,[47] A. M. Poskanzer,[22] M. Potekhin,[3] E. Potrebenikova,[12] B. V. K. S. Potukuchi,[19] D. Prindle,[47] C. Pruneau,[48] J. Putschke,[22] G. Rakness,[31] R. Raniwala,[35] S. Raniwala,[35] R. L. Ray,[42] S. V. Razin,[12] J. Reinnarth,[40] D. Relyea,[4] F. Retiere,[22] A. Ridiger,[26] H. G. Ritter,[22] J. B. Roberts,[36] O. V. Rogachevskiy,[12] J. L. Romero,[6] A. Rose,[22] C. Roy,[40] L. Ruan,[22] M. J. Russcher,[28] R. Sahoo,[15] T. Sakuma,[23] S. Salur,[50] J. Sandweiss,[50] M. Sarsour,[41] P. S. Sazhin,[12] J. Schambach,[42] R. P. Scharenberg,[33] N. Schmitz,[24] K. Schweda,[22] J. Seger,[10] I. Selyuzhenkov,[48] P. Seyboth,[24] A. Shabetai,[20] E. Shahaliev,[12] M. Shao,[38] M. Sharma,[30] W. Q. Shen,[39] S. S. Shimanskiy,[12] E Sichtermann,[22] F. Simon,[23] R. N. Singaraju,[45] N. Smirnov,[50] R. Snellings,[28] G. Sood,[44] P. Sorensen,[3] J. Sowinski,[17] J. Speltz,[18] H. M. Spinka,[1] B. Srivastava,[33] A. Stadnik,[12] T. D. S. Stanislaus,[44] R. Stock,[14] A. Stolpovsky,[48] M. Strikhanov,[26] B. Stringfellow,[33] A. A. P. Suaide,[37] E. Sugarbaker,[29] M. Sumbera,[11] Z. Sun,[21] B. Surrow,[23] M. Swanger,[10] T. J. M. Symons,[22] A. Szanto de Toledo,[37] A. Tai,[7] J. Takahashi,[37] A. H. Tang,[3] T. Tarnowsky,[33] D. Thein,[7] J. H. Thomas,[22] A. R. Timmins,[2] S. Timoshenko,[26] M. Tokarev,[12] T. A. Trainor,[47] S. Trentalange,[7] R. E. Tribble,[41] O. D. Tsai,[7] J. Ulery,[33] T. Ullrich,[3] D. G. Underwood,[1] G. Van Buren,[3] N. van der Kolk,[28] M. van Leeuwen,[22] A. M. Vander Molen,[25] R. Varma,[16] I. M. Vasilevski,[13] A. N. Vasiliev,[32] R. Vernet,[18] S. E. Vigdor,[17] Y. P. Viyogi,[15] S. Vokal,[12] S. A. Voloshin,[48] W. T. Waggoner,[10] F. Wang,[33] G. Wang,[7] J. S. Wang,[21] X. L. Wang,[38] Y. Wang,[43] J. W. Watson,[20] J. C. Webb,[44] G. D. Westfall,[25] A. Wetzler,[22] C. Whitten, Jr.,[7] H. Wieman,[22] S. W. Wissink,[17] R. Witt,[50] J. Wood,[7] J. Wu,[38] N. Xu,[22] Q. H. Xu,[22] Z. Xu,[3] P. Yepes,[36] I-K. Yoo,[34] V. I. Yurevich,[12] W. Zhan,[21] H. Zhang,[3] W. M. Zhang,[20] Y. Zhang,[38] Z. P. Zhang,[38] Y. Zhao,[38] C. Zhong,[39] R. Zoulkarneev,[13] Y. Zoulkarneeva,[13] A. N. Zubarev,[12] and J. X. Zuo[39]

132301-1

(STAR Collaboration)

[1]Argonne National Laboratory, Argonne, Illinois 60439, USA
[2]University of Birmingham, Birmingham, United Kingdom
[3]Brookhaven National Laboratory, Upton, New York 11973, USA
[4]California Institute of Technology, Pasadena, California 91125, USA
[5]University of California, Berkeley, California 94720, USA
[6]University of California, Davis, California 95616, USA
[7]University of California, Los Angeles, California 90095, USA
[8]Carnegie Mellon University, Pittsburgh, Pennsylvania 15213, USA
[9]University of Illinois, Chicago
[10]Creighton University, Omaha, Nebraska 68178, USA
[11]Nuclear Physics Institute AS CR, 250 68 Řež/Prague, Czech Republic
[12]Laboratory for High Energy (JINR), Dubna, Russia
[13]Particle Physics Laboratory (JINR), Dubna, Russia
[14]University of Frankfurt, Frankfurt, Germany
[15]Institute of Physics, Bhubaneswar 751005, India
[16]Indian Institute of Technology, Mumbai, India
[17]Indiana University, Bloomington, Indiana 47408, USA
[18]Institut de Recherches Subatomiques, Strasbourg, France
[19]University of Jammu, Jammu 180001, India
[20]Kent State University, Kent, Ohio 44242, USA
[21]Institute of Modern Physics, Lanzhou, China
[22]Lawrence Berkeley National Laboratory, Berkeley, California 94720, USA
[23]Massachusetts Institute of Technology, Cambridge, Massachusetts 02139-4307, USA
[24]Max-Planck-Institut für Physik, Munich, Germany
[25]Michigan State University, East Lansing, Michigan 48824, USA
[26]Moscow Engineering Physics Institute, Moscow Russia
[27]City College of New York, New York City, New York 10031, USA
[28]NIKHEF and Utrecht University, Amsterdam, The Netherlands
[29]Ohio State University, Columbus, Ohio 43210, USA
[30]Panjab University, Chandigarh 160014, India
[31]Pennsylvania State University, University Park, Pennsylvania 16802, USA
[32]Institute of High Energy Physics, Protvino, Russia
[33]Purdue University, West Lafayette, Indiana 47907, USA
[34]Pusan National University, Pusan, Republic of Korea
[35]University of Rajasthan, Jaipur 302004, India
[36]Rice University, Houston, Texas 77251, USA
[37]Universidade de Sao Paulo, Sao Paulo, Brazil
[38]University of Science & Technology of China, Hefei 230026, China
[39]Shanghai Institute of Applied Physics, Shanghai 201800, China
[40]SUBATECH, Nantes, France
[41]Texas A&M University, College Station, Texas 77843, USA
[42]University of Texas, Austin, Texas 78712, USA
[43]Tsinghua University, Beijing 100084, China
[44]Valparaiso University, Valparaiso, Indiana 46383, USA
[45]Variable Energy Cyclotron Centre, Kolkata 700064, India
[46]Warsaw University of Technology, Warsaw, Poland
[47]University of Washington, Seattle, Washington 98195, USA
[48]Wayne State University, Detroit, Michigan 48201, USA
[49]Institute of Particle Physics, CCNU (HZNU), Wuhan 430079, China
[50]Yale University, New Haven, Connecticut 06520, USA
[51]University of Zagreb, Zagreb, HR-10002, Croatia

We report the measurements of $\Sigma(1385)$ and $\Lambda(1520)$ production in $p + p$ and Au + Au collisions at $\sqrt{s_{NN}} = 200$ GeV from the STAR Collaboration. The yields and the p_T spectra are presented and discussed in terms of chemical and thermal freeze-out conditions and compared to model predictions. Thermal and microscopic models do not adequately describe the yields of all the resonances produced in

central Au + Au collisions. Our results indicate that there may be a time span between chemical and thermal freeze-out during which elastic hadronic interactions occur.

In ultrarelativistic heavy-ion collisions, hot and dense nuclear matter (a fireball) is created [1,2]. When the energy density of the created fireball is very high, deconfinement of partons is expected to occur and a new phase of matter, the quark gluon plasma (QGP) forms. After hadronization of the QGP, but before the interactions of the hadrons cease, the physical properties of resonances, such as their *in vacuo* masses and widths, might be modified by the density of the surrounding nuclear medium [3]. In addition, the yield of resonances might change.

The temperature and the density of the fireball reduces as the fireball expands. Chemical freezeout is reached when hadrons stop interacting inelastically. Elastic interactions continue until thermal freezeout. Because of their short lifetimes, a fraction of resonances can decay before the thermal freezeout. Elastic interactions of the decay products with other particles in the medium (rescattering) may modify their momenta enough that the parent particle can no longer be identified. The pseudoelastic hadronic interactions (regeneration) may increase the resonance yields [e.g., $\Lambda + \pi \leftrightarrow \Sigma^*(1385)$] [4–7]. The overall net effect of rescattering and regeneration on the total observed yields depends on the time span between chemical and thermal freezeout, the lifetime of the resonances and the magnitudes of the interaction cross sections of the decay particles [8,9]. Thermal models provide the resonance to stable particle ratios at the chemical freezeout. Deviations from these predicted ratios due to rescattering of the resonance decay particles can be used to estimate the time span between chemical and thermal freezeout.

We report on the first measurements of the production of the $\Sigma^*(1385)$ [10] and $\Lambda(1520)$ [11] in $p + p$ and Au + Au collisions at $\sqrt{s_{NN}} = 200$ GeV. The effects of the extended nuclear medium on the resonance yields and momentum spectra are studied by comparing those results from the different collision systems. Microscopic transport [4] and thermal [12–14] models are used to investigate the time span of hadronically interacting phase.

The STAR detector system [15], with its large time projection chamber (TPC), is used to identify the decay products of the $\Sigma(1385) \rightarrow \Lambda + \pi$ and $\Lambda(1520) \rightarrow p + K$. For Au + Au collisions, the number of charged particles in the TPC is used to select the centrality of inelastic interactions. Different y and centrality selections are necessary for $\Sigma(1385)$ and $\Lambda(1520)$ in order to optimize the statistical significance of each measurement.

The topological reconstruction of resonance decay vertices is not possible due to their short lifetimes resulting from their strong decay. Instead an invariant mass calculation from the decay daughter candidates is performed. Charged particles are identified by the energy loss per unit length, dE/dx, and the momentum measured with the TPC. The decay topology information is used to identify the neutral Λ [16]. A large source of background in the invariant mass spectra for both $\Sigma(1385)$ and $\Lambda(1520)$ comes from uncorrelated pairs. A mixed-event technique, where no correlations are possible, is used to estimate the contribution of the background [17]. The background is normalized over a wide kinematic range and then subtracted from the invariant mass distribution. For the $\Sigma^-(1385)$, a Ξ^- peak remains as it has the same $\Lambda + \pi^-$ decay channel. In order to enhance the statistics for the Σ^*, two charged channels are combined [$\Sigma^\pm(1385)$] for $p\pi^+ + p\pi^-$ and all four charged channels [$\Sigma^\pm(1385) + $
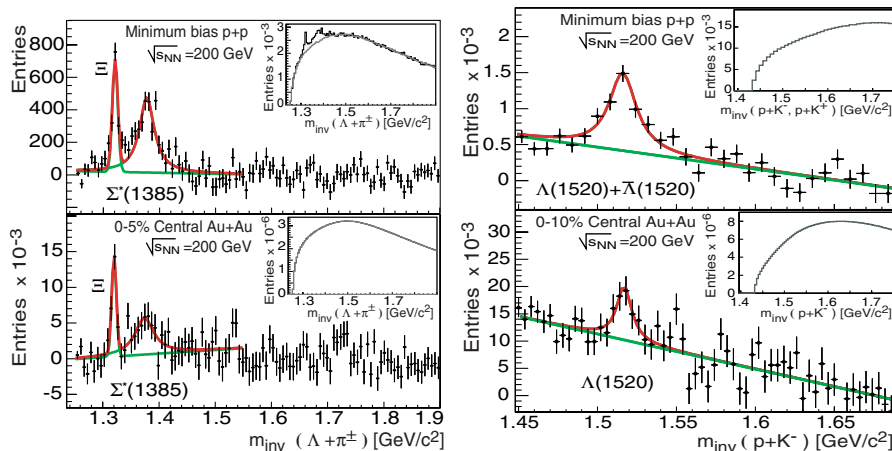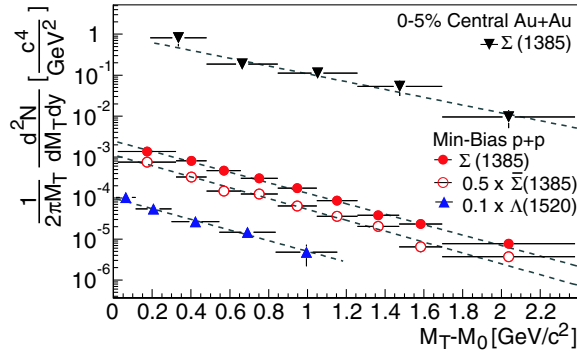

FIG. 1 (color online). Invariant mass distributions of Σ^* and Λ^* in $p + p$ and Au + Au collisions at $\sqrt{s_{NN}} = 200$ GeV before (inset) and after mixed-event background subtraction.

TABLE I. Mass (M) and width (Γ) fit parameters of particles from Fig. 1, including statistical and systematic errors.

Particle	M [MeV/c^2]	Γ [MeV/c^2]	p_T [GeV/c]	$|y|$
$\Xi^-_{(p+p)}$	$1320 \pm 1 \pm 1$	$7 \pm 1 \pm 1$	0.25–3.50	≤ 0.75
$\Xi^-_{(Au+Au)}$	$1320 \pm 1 \pm 1$	$4 \pm 1 \pm 1$	0.50–3.50	≤ 0.75
$\Xi^*_{(p+p)}$	$1376 \pm 3 \pm 3$	$44 \pm 8 \pm 8$	0.25–3.50	≤ 0.75
$\Xi^*_{(Au+Au)}$	$1375 \pm 5 \pm 3$	$43 \pm 5 \pm 6$	0.50–3.50	≤ 0.75
$\Lambda^*_{(p+p)}$	$1516 \pm 2 \pm 2$	$20 \pm 4 \pm 2$	0.20–2.20	≤ 0.50
$\Lambda^*_{(Au+Au)}$	$1516 \pm 2 \pm 2$	$12 \pm 6 \pm 3$	0.90–2.00	≤ 1.00

FIG. 2 (color online). The transverse mass spectra for Ξ^* and Λ^* in $p + p$ and in central Au + Au collisions at $\sqrt{s_{NN}} = 200$ GeV. Statistical and systematical errors are included.

$\bar{\Sigma}^{\pm}(1385)$] for Au + Au collisions. Similarly for the Λ^*, $\Lambda(1520)$ and $\bar{\Lambda}(1520)$ are combined in $p + p$ collisions. As the $\bar{\Lambda}(1520)$ is not observed in central Au + Au collisions, it is not included in our definition of Λ^* in Au + Au.

Figure 1 shows the invariant mass distributions for Ξ^* and Λ^* in 10×10^6 minimum bias $p + p$ and 1.6×10^6 central Au + Au collisions. The mass (M) and the width (Γ) fit parameters of the measured transverse momentum (p_T) and rapidity (y) ranges are shown in Table I. These parameters and their uncertainties are obtained from combined fits. A Gaussian distribution takes into account the detector resolution effects on the Ξ^-. Since the natural width dominates over the detector resolutions for both the Ξ^* and Λ^*, a nonrelativistic Breit-Wigner distribution is used. Finally, the remaining residual background is described by a linear function. The measured widths, taking into account the detector resolution, are, within their uncertainties, in agreement with the PDG [18]. The observed mass and the width of the Ξ^- peak is in agreement with the one obtained via the topological method [16]. While the masses of Ξ^* and Λ^* are also in agreement with the PDG values, there is a small difference in the mass of the Ξ^*. Because of limited statistics, it is not possible to investigate this effect further. The systematic errors include the uncertainty due to bin size fluctuations, the normalization of the mixed-event background and the uncertainty of the straight line fit range due to correlations in misidentified decay particles. Event and track selections were also varied.

To obtain the integrated raw yields of Ξ^* and Λ^*, the background subtracted invariant mass spectrum in each p_T bin is fitted. In the corresponding mass range, the content of each bin above the linear background fit is counted to extract the raw yields. Monte Carlo simulated resonances are embedded into real $p + p$ and Au + Au events to determine the correction factors for the detector acceptance and reconstruction efficiency. These are applied to the data and the corrected transverse mass spectra of Ξ^* and Λ^* in $p + p$ and Au + Au collisions are shown in Fig. 2. The dashed curves represent an exponential fit to the data [17]. The mean p_T ($\langle p_T \rangle$) and the yields at midrapidity (dN/dy) as obtained from the fit are listed in Table II together with their corresponding statistical uncertainties. The yields are obtained by extrapolating the fit to all p_T. The measured p_T range contains 85% for Ξ^* and 50% for Λ^* in Au + Au and 91% for Ξ^* and Λ^* in $p + p$ of the total midrapidity yields. For Λ^*, due to the low statistics in Au + Au collisions, an inverse slope of $T = 400$ MeV is assumed in order to extract the particle yield. The systematic error includes a $\Delta T = 100$ MeV variation. The ratio of $\bar{\Lambda}^*/\Lambda^* = 0.93 \pm 0.11$ in $p + p$ collisions is extracted from the corrected yields. Statistical limitations require that the $\bar{\Xi}^*/\Xi^* = 0.87 \pm 0.18$ in Au + Au collisions are determined from the raw yields. The proximity of these ratios to unity, reflects a small net baryon number at midrapidity of both systems.

A linear increase of $\langle p_T \rangle$ as a function of particle mass up to 1 GeV/c^2 is observed in Au + Au and $p + p$ collisions [16,19]. The measured $\langle p_T \rangle$ of Ξ^* and Λ^* in $p + p$ collisions follow a steeper increase, similar to the trend of heavier mass particles (> 1 GeV/c^2). This might be due

TABLE II. $\langle p_T \rangle$ and yields from fits to the p_T spectra, dN/dy for Λ^* in Au + Au using a fixed T. The $p + p$ yields are from nonsingly diffractive collisions. Ξ^* represents $\Xi^{*+} + \Xi^{*-}$.

Particle	Collision	$\langle p_T \rangle$ [GeV/c]	$(dN/dy)\|_{y=0}$
Ξ^*	pp_{minbias}	$1.02 \pm 0.02 \pm 0.07$	$(10.7 \pm 0.4 \pm 1.4) \times 10^{-3}$
$\bar{\Xi}^*$	pp_{minbias}	$1.01 \pm 0.01 \pm 0.06$	$(8.9 \pm 0.4 \pm 1.2) \times 10^{-3}$
$\bar{\Xi}^* + \Xi^*$	$AuAu_{0\%-5\%}$	$1.28 \pm 0.15 \pm 0.09$	$9.3 \pm 1.4 \pm 1.2$
$\bar{\Lambda}^* + \Lambda^*$	pp_{minbias}	$1.08 \pm 0.09 \pm 0.05$	$(6.9 \pm 0.5 \pm 1.0) \times 10^{-3}$
Λ^*	$AuAu_{0\%-10\%}$	$1.20 \pm 0.20_{\text{fixed}}$	$(6.3 \pm 2.1 \pm 0.8) \times 10^{-1}$
$\bar{\Lambda}^* + \Lambda^*$	$AuAu_{60\%-80\%}$	$1.20 \pm 0.20_{\text{fixed}}$	$(8.9 \pm 2.9 \pm 1.1) \times 10^{-2}$

to the fact that the higher mass particles come from events with average multiplicities a factor of 2 or more higher than those for the minimum bias events. The increase in the $\langle p_T \rangle$ and the larger event multiplicities imply that these resonances come from mini-jet-like events [20]. The rescattering and regeneration is expected to change the $\langle p_T \rangle$ in Au + Au collisions. However, it is surprising that the $\langle p_T \rangle$ of *in p + p and Au + Au collisions are in agreement within their uncertainties.

The ratios of yields of resonances to stable particles as a function of the charged particle multiplicity are presented in Fig. 3. The ratios are normalized to unity in p + p collisions to study variations in Au + Au relative to p + p. We measure a suppression for Λ^*/Λ when comparing central Au + Au with minimum bias p + p. K^*/K^- [17] seems to show a smaller suppression while the $*/\Lambda$, and ϕ/K^- [21] ratios are consistent with unity. In a thermal model, the measured ratios of resonance to nonresonant particles with identical valence quarks are particularly sensitive to the chemical freezeout temperature, as all of the quark content dependencies cancel out. Thermal models require a chemical freezeout temperature in the range $T_{ch} = 160$–180 MeV and a baryo-chemical potential $\mu_B = 20$–50 MeV in 200 GeV Au + Au collisions to describe the stable particle ratios [12,13]. While these models predict the measured $*/\Lambda$ ratio correctly within the errors, they yield a higher ratio than the measured Λ^*/Λ in the most central Au + Au collisions. This suggests an extended hadronic phase of elastic and pseudoelastic interactions after chemical freezeout, where rescattering of resonance decay particles and regeneration of resonances will occur. The measured resonance yields thus depend on the time span between chemical and kinetic freezeout, their cross sections for rescattering and regeneration, and their lifetimes. The suppressed Λ^*/Λ and K^*/K^- ratios in

Au + Au suggest that rescattering dominates regeneration in the hadronic medium after chemical freezeout.

A thermal model using an additional pure rescattering phase, which depends on the respective momenta of the resonance decay products, after chemical freezeout at $T_{ch} = 160$ MeV, can be fit to the data. The fit yields a hadronic lifetime of the source of $\tau = 9^{+10}_{-5}$ fm/c from the Λ^*/Λ and $\tau = 2.5^{+1.5}_{-1}$ fm/c from the K^*/K ratio [9,22]. The small difference between the time spans can be explained by an enhanced regeneration cross section for the K^* in the medium. This theory is supported by the null suppression of the $*/\Lambda$. The smaller lifetime of the $*$ compared to the Λ^* should lead to a larger signal loss due to rescattering, thus the lack of suppression requires an enhanced regeneration probability of the $*$. Based on the same argument the K^* regeneration cross section needs to be larger than that of the Λ^* due to the observed smaller suppression and shorter lifetime of the K^* (i.e., defining R as the ratio of regeneration to rescattering cross section, we find $R_{K+p} < R_{K+\pi} < R_{\Lambda+\pi}$ since $c\tau_{K^*} < c\tau_\psi < c\tau_{\Lambda^*}$). A microscopic model calculation (UrQMD) with a typical lifespan of $\tau = 3 \pm 3$ fm/c for the rescattering and regeneration phase, can describe K^*/K^- and Λ^*/Λ ratios approximately, but fails for the $*/\Lambda$ [8]. The measured resonance yields in heavy-ion collisions provide a tool to determine the strength of in-medium hadronic cross sections and current microscopic transport models such as UrQMD will have to be modified to account for such cross sections [23]. The τ extracted from the measurements can be used in comparison to the analysis of two-pion intensity interferometry (HBT) in order to obtain an estimate for the partonic lifetime. Identical particle HBT yields a time of 5–12 fm/c from the start of the collision to the kinetic freezeout (total source lifetime) [24]. If one assumes the Λ^* to be least affected by regeneration then the extracted $\tau > 4$ fm/c is a lower limit on the hadronic source lifetime, which is a subinterval of the total source lifetime. The remaining time would be a rough estimate on the partonic lifetime of the source.

Although the rescattering and regeneration scheme is discussed predominantly, other methods to describe the data have been proposed. For example, in a sudden freezeout scenario, where the time between the chemical and kinetic freezeout is negligible, the Λ^*/Λ suppression in Au + Au with respect to p + p can be explained by the influence of the dense medium on the production of Λ^*. Even though the valence quarks of the Λ^* are in a $L = 1$ state, it must decay through a relative angular momentum $L = 2$ process in order to conserve isospin [25]. The high partial wave component of the Λ^* in a dense medium can suppress its decay phase space.

We have presented the first measurements of $*$ and Λ^* production in p + p and Au + Au collisions at $\sqrt{s_{NN}} = 200$ GeV. The large $\langle p_T \rangle$ of the $*$ and Λ^* measurements in p + p collisions suggests that the heavy particle pro-
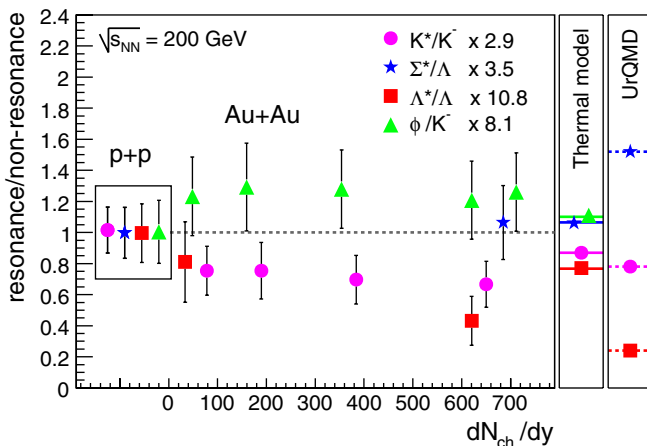
FIG. 3 (color online). Resonance to stable particle ratios for p + p and Au + Au collisions. The ratios are normalized to unity in p + p and compared to thermal and UrQMD model predictions for central Au + Au [8,12]. Statistical and systematic uncertainties are included in the error bars.

duction receives a significant contribution from jetlike events. The yields of *, Λ^*, ϕ and K^* in Au + Au in comparison to $p + p$ collisions indicate the presence of rescattering and regeneration for a nonzero time span between chemical and kinetic freezeout. A lower limit for the hadronic source lifetime of $\tau > 4$ fm/c is estimated based on a thermal model including rescattering.

[1] K. Adcox *et al.*, Phys. Rev. Lett. **87**, 052301 (2001).
[2] J. Adams *et al.*, Phys. Rev. Lett. **92**, 112301 (2004).
[3] M. F. M. Lutz *et al.*, Nucl. Phys. **A700**, 193 (2002).
[4] S. A. Bass *et al.*, Phys. Rev. C **61**, 064909 (2000).
[5] R. Rapp *et al.*, Phys. Rev. Lett. **86**, 2980 (2001).
[6] H. van Hees *et al.*, Phys. Lett. B **606**, 59 (2005).
[7] C. Adler *et al.*, Phys. Rev. C **66**, 061901 (2002).
[8] M. Bleicher *et al.*, Phys. Lett. B **530**, 81 (2002); M. Bleicher, Nucl. Phys. **A715**, 85 (2003).
[9] G. Torrieri *et al.*, Phys. Lett. B **509**, 239 (2001); J. Rafelski *et al.*, Phys. Rev. C **64**, 054907 (2001); J. Rafelski *et al.*, Phys. Rev. C **65**, 069902 (2002).
[10] S. Salur, Ph.D. thesis, Yale University, 2006.
[11] L. Gaudichet, Ph.D. thesis, Nantes University, 2003.
[12] P. Braun-Munzinger *et al.* Phys. Lett. B **518**, 41 (2001).
[13] F. Becattini, Nucl. Phys. **A702**, 336 (2002).
[14] J. Adams *et al.*, Nucl. Phys. **A757**, 102 (2005).
[15] M. Anderson *et al.*, Nucl. Instrum. Methods Phys. Res., Sect. A **499**, 659 (2003).
[16] J. Adams *et al.*, nucl-ex/0601042.
[17] J. Adams *et al.*, Phys. Rev. C **71**, 064902 (2005).
[18] S. Eidelman *et al.*, Phys. Lett. B **592** 1 (2004).
[19] B. Abelev *et al.*, nucl-ex/0607033.
[20] A. Dumitru *et al.*, Phys. Lett. B **446**, 326 (1999).
[21] J. Adams *et al.*, Phys. Lett. B **612**, 181 (2005).
[22] C. Markert *et al.*, hep-ph/0206260.
[23] S. Vogel *et al.*, hep-ph/0607242.
[24] J. Adams *et al.*, Phys. Rev. C **71**, 044906 (2005).
[25] M. Kaskulov *et al.*, Phys. Rev. C **73**, 045213 (2006).